

Electronic density of states and the x-ray photoelectron spectra of the valence band of Cu-Pd alloys

H. Winter

*Institut für Technische Physik, Kerforschungszentrum Karlsruhe, Postfach 3640,
D-7500 Karlsruhe, Federal Republic of Germany*

P. J. Durham and W. M. Temmerman

*Daresbury Laboratory, United Kingdom Science and Engineering Research Council, Daresbury,
Warrington WA4 4AD, United Kingdom*

G. M. Stocks

Oak Ridge National Laboratory, Oak Ridge, Tennessee 37831

(Received 26 April 1984; revised manuscript received 28 January 1985)

We present self-consistent-field Korringa-Kohn-Rostoker coherent-potential-approximation calculations of the electronic density of states of random $\text{Cu}_c\text{Pd}_{1-c}$ alloys. We find strong hybridization of the palladium d bands with the copper d bands over the entire concentration range. We do not obtain a palladium virtual bound state for the copper-rich alloys and therefore contradict the interpretation generally placed on valence-band x-ray photoelectron spectroscopy (XPS) spectra for Cu-Pd. Nevertheless, our first-principles calculations of the XPS spectra are in excellent agreement with recent measurements, and we discuss why this is so. Furthermore, we compare our density of states at the Fermi energy with specific-heat measurements.

I. INTRODUCTION

X-ray photoelectron spectroscopy (XPS) has been extensively applied to the valence bands of disordered transition- and noble-metal alloys (and glasses) in order to establish the main features of the d -band densities of states. For example, in Cu-Ni and Ag-Pd alloys XPS spectra show two sets of d states, directly confirming the split-band picture. In Cu (Ag)-rich alloys the Ni (Pd) d levels form virtual bound states above the host d bands that are centered on the d -scattering resonances of the impurity. The many XPS measurements¹⁻⁵ on Cu-Pd alloys are less clear-cut, but here too the interpretation of the data has always been, with the exception of Ref. 5, that a palladium virtual bound state is formed in copper-rich alloys. In this paper we present the first self-consistent-field Korringa-Kohn-Rostoker coherent-potential-approximation (KKR-CPA) calculations of the densities of states in Cu-Pd alloys. Although the KKR-CPA leads to Ni (Pd) virtual bound states in Cu-Ni and Ag-Pd alloys, we show that Cu-Pd behaves quite differently. In tight-binding terms we characterize Cu-Pd as a system in which off-diagonal disorder dominates diagonal disorder. It is the first such system to be analyzed using the KKR-CPA, and a number of novel features appear in the density of states. The most striking effect, however, is that there is a common d band at all concentrations and no palladium virtual bound state. Rather, the Pd d density of states has two peaks, one each at the upper and lower Cu d -band edges. This finding is in agreement with the results of recent non-self-consistent KKR-CPA calculations for two Cu-rich Cu-Pd alloys by Rao *et al.*,⁶ the crystal potentials for which were adjusted empirically to

force consistency with experimental angle-resolved photoemission data. In addition to performing the self-consistent-field calculations, we have made first-principles calculations of the XPS spectra, according to the one-electron theory we advanced in an earlier paper,⁷ and obtain very satisfactory agreement with experiment. Therefore, we believe previous interpretations^{3,4} of the data to have been wrong, and we point out the origin of this error. We also discuss the electronic specific-heat coefficient γ and electron-phonon mass enhancement λ in the light of our calculations of $n(\epsilon_F)$ and comment on the tendency towards superconductivity in this alloy.

Copper and palladium form random alloys of fcc structure (α phase) at temperatures above 600 K throughout the concentration range. This structure persists to low temperature, except for palladium concentrations between about 10% and 25%, where transformations into the Cu_3Au structure and into long-period ordered structures occur, and between 30% and 50%, where transformations into the CsCl structure occur.⁸ However, using rapid-quenching techniques it is possible to maintain the α phase at low temperatures throughout the concentration range.^{4,9} In spite of the propensity of these alloys to establish some degree of short-range order, as has been demonstrated by diffuse electron scattering work,¹⁰ it seems reasonable, as a first step, to calculate the electronic structure of the $\text{Cu}_c\text{Pd}_{1-c}$ alloy system under the assumption of complete randomness. Even if the physical quantity in question depends non-negligibly on ordering or clustering effects, the results for the random case are needed as the starting point for taking into account such effects.¹¹⁻¹³

Unlike $\text{Ag}_c\text{Pd}_{1-c}$ and $\text{Cu}_c\text{Ni}_{1-c}$, $\text{Cu}_c\text{Pd}_{1-c}$ alloys con-

sist of atoms belonging to different series in the periodic table and thus differ significantly in atomic number. As a result it is difficult to construct reliable alloy potential function by the standard method of superimposing atomic charge densities.¹⁴ This difficulty was overcome in the work of Rao *et al.* by the introduction of a rigid shift of the Pd-site potential with respect to the Cu-site potential by 2.45 eV, and a shift of the Cu *d* band with respect to the *sp* bands of 0.15 eV. The reason for the difficulty is because for potentials constructed from overlapping atomic charge densities the Wigner-Seitz cells corresponding to copper and to palladium sites in the alloy turn out to be far from neutral. In the case of $\text{Cu}_{0.75}\text{Pd}_{0.25}$ about one electronic charge is missing at the palladium site. Thus for $\text{Cu}_c\text{Pd}_{1-c}$ alloys it is necessary that the calculations be made self-consistent with respect to the alloy potential in order to obtain alloy-crystal potentials which will give an accurate description of the electronic structure that is completely parameter free, eliminating the necessity of empirical adjustment. This is in contrast to $\text{Ag}_c\text{Pd}_{1-c}$ (Ref. 15) and $\text{Cu}_c\text{Ni}_{1-c}$ (Refs. 16 and 17), where electronic structure calculations based on Mattheiss-prescription potentials yield reasonable results. Inspection of the pure Cu and Pd band structures leads one to expect substantial Cu and Pd *d*-band mixing in the alloy. The pure Cu and Pd *d*-band widths are very different, being, respectively, 3.3 and 5.5 eV. Furthermore, the change of the lattice constants that occurs when Cu and Pd are alloyed tends to accentuate this difference. The lattice contracts on the addition of palladium, which results in a broadening of the palladium band and a narrowing of the copper band. In contrast, the lattice-constant changes that occur on alloying Ag and Pd tend to equalize the Ag and Pd *d*-band widths.¹⁴ The lattice expands on alloying Ag to Pd, narrowing the palladium *d* band and broadening the silver *d* band. In this paper we will investigate, in detail, the effects of self-consistency and the consequences of the large difference in bandwidth of the alloy constituents on the electronic density of states.

Sato *et al.*¹⁸ measured the low-temperature specific heat of the α phase alloys throughout the concentration range. In the concentration range where the alloys are metastable with respect to the formation of the β bcc phase, they estimate the values by interpolation except for the composition $\text{Cu}_{0.59}\text{Pd}_{0.41}$, for which they produced samples of both fcc and CsCl structure. The Debye frequency extracted from the phonon part of the specific heat decreases monotonically from the copper-rich to the palladium-rich end. The electronic specific-heat coefficient γ shows a steep rise with increasing palladium concentration starting at about 40% palladium. Below this value it is only weakly concentration dependent. This observation led to the conclusion that, on alloying, the 0.6 holes in the palladium *d* band are filled up by copper *s* electrons at 60% copper.

Other experimental studies include NMR measurements of Knight shifts and relaxation times at the copper sites.^{19–21} It is found that beyond 40% of palladium the Knight shift scales with the average susceptibility. From this it was concluded that the Fermi energy enters the *d* bands at 40% palladium in $\text{Cu}_c\text{Pd}_{1-c}$.

We have calculated the electronic structure of the $\text{Cu}_c\text{Pd}_{1-c}$ alloys within the KKR-CPA.^{16,22} Self-consistency with respect to the alloy potential has been obtained along the lines described by Winter and Stocks.^{23,24} The XPS valence-band spectra are evaluated within a one-particle approximation.⁷ Our calculated densities of states for $\text{Cu}_{0.75}\text{Pd}_{0.25}$ and $\text{Cu}_{0.95}\text{Pd}_{0.05}$ have already been used to interpret Auger measurements as well as XPS data for these alloys,⁵ where it was pointed out that neither the Auger nor the XPS measurements supported a split-band picture for these alloys. Gyroffy and Stocks¹³ used the self-consistent electronic structure calculations as a basis for investigating the driving force responsible for the formation of concentration waves that are observed in the disordered α phase alloys.¹⁰ A concentration wave may be thought of as a long-lived periodic fluctuation in the site concentration about the homogeneous (random) alloy. The driving mechanism they proposed is the nesting of flat pieces of Fermi surface. The length and direction of the spanning vectors that connect the flat sheets of Fermi surface are directly related to the positions of the diffuse scattering peaks found in electron scattering experiments.¹⁰ The electron-positron momentum distribution for $\text{Cu}_{0.60}\text{Pd}_{0.40}$ has also been calculated from our self-consistent charge densities.²⁵

The Cu-Pd system therefore exhibits a range of interesting physical behavior and has attracted a good deal of experimental activity. However, before attempting to construct a detailed microscopic description of its properties, it is essential to establish the general features of the electronic structure of Cu-Pd. This is the purpose of the present paper.

In Sec. II we discuss our results for the electronic density of states of $\text{Cu}_{0.95}\text{Pd}_{0.05}$, $\text{Cu}_{0.75}\text{Pd}_{0.25}$, $\text{Cu}_{0.60}\text{Pd}_{0.40}$, $\text{Cu}_{0.50}\text{Pd}_{0.50}$, $\text{Cu}_{0.25}\text{Pd}_{0.75}$, and $\text{Cu}_{0.10}\text{Pd}_{0.90}$. In Sec. III our calculated XPS spectra are compared with the experimental results. In Sec. IV we draw conclusions.

II. THE ELECTRONIC STRUCTURE

The self-consistent-field (SCF) alloy potentials were obtained by the cluster method of solving the CPA equations described previously.^{23,24} The cluster size was 79 atoms and the von Barth–Hedin²⁶ exchange and correlation potential was used. The densities of states were obtained after one final iteration with the full KKR-CPA,¹⁷ which left the self-consistent cluster charge density unchanged, thereby confirming the adequacy of the use of the cluster method.

In contrast to Ag-Pd alloys,^{23,24} we find, for the whole concentration range, that the palladium *d* resonance is *below* the copper *d* resonance (Fig. 1). That this is the case appears to follow from our finding that Cu and Pd Wigner-Seitz cells are essentially charge neutral (Table I), the point being that, in this alloy system, the palladium *d* resonance is rather wide; thus, in order for it to hold sufficient electrons to ensure neutrality, it must lie low in energy.

Figures 2–7 show the densities of states for $\text{Cu}_{0.95}\text{Pd}_{0.05}$, $\text{Cu}_{0.75}\text{Pd}_{0.25}$, $\text{Cu}_{0.60}\text{Pd}_{0.40}$, $\text{Cu}_{0.50}\text{Pd}_{0.50}$, $\text{Cu}_{0.25}\text{Pd}_{0.75}$, and $\text{Cu}_{0.10}\text{Pd}_{0.90}$, respectively. The upper left-hand panel gives the total density of states and its

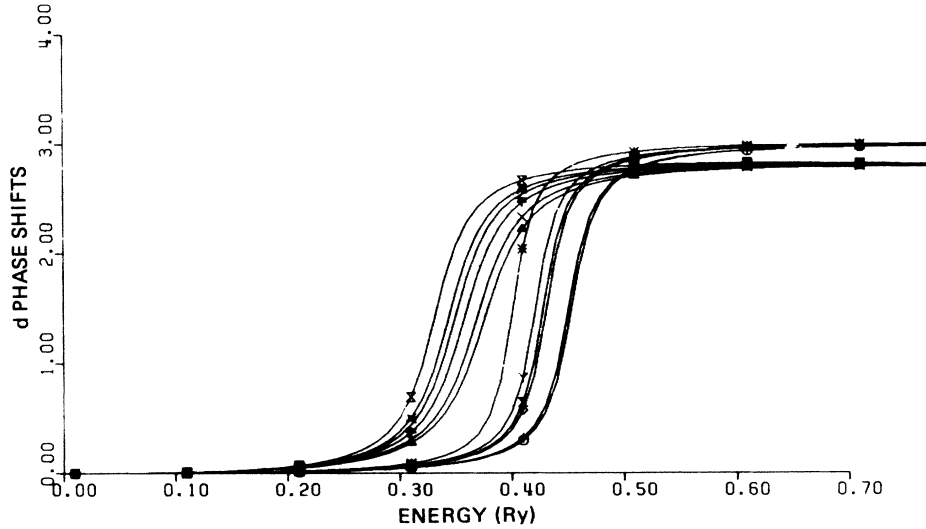


FIG. 1. Cu-site and Pd-site d -wave phase shifts for the self-consistent alloy potentials for six different alloy compositions. The group of six curves having the lowest resonance energy ($\eta_2 = \pi/2$) are for the Pd-sites; the remaining six are for the Cu-sites. Within each group, in order of increasing resonance energy, the curves are for $\text{Cu}_{0.95}\text{Pd}_{0.05}$, $\text{Cu}_{0.75}\text{Pd}_{0.25}$, $\text{Cu}_{0.60}\text{Pd}_{0.40}$, $\text{Cu}_{0.5}\text{Pd}_{0.5}$, $\text{Cu}_{0.25}\text{Pd}_{0.75}$, and $\text{Cu}_{0.10}\text{Pd}_{0.90}$ alloys.

decomposition into concentration-weighted partial densities of states; in the upper and lower right-hand panels the partial densities of states are displayed. We find a common d band for the whole concentration range in rough agreement with the empirically adjusted results of Rao *et al.* The d band moves closer to the Fermi energy and becomes wider with increasing palladium concentration. The high density of states of the copper d bands decreases continuously.

From panels displaying the total density of states, we see that there are always Cu and Pd states over the whole energy range of the d band: Hybridization of Pd with Cu has introduced new states on the copper sites toward the bottom of the d bands—the bands which are of predominantly bonding character. We can quantify this by determining the energy width of the total density of states at five states per Ry atom spin (W_2) and at ten states per Ry atom spin (W_1). While for alloys with up to 50% of palladium W_1 remains equal to 2.9 eV, W_2 increases from 4.0 eV (5% Pd), 4.9 eV (25% Pd), and 5.2 eV (40% Pd), to 5.3 eV (50% Pd). For $\text{Cu}_{0.25}\text{Pd}_{0.75}$ and

$\text{Cu}_{0.10}\text{Pd}_{0.90}$ those states at the bottom of the d band now have more than ten states per Ry atom spin and W_1 and W_2 have become comparable: 5.0 and 5.7 eV for $\text{Cu}_{0.25}\text{Pd}_{0.75}$ and 5.2 and 5.8 eV for $\text{Cu}_{0.10}\text{Pd}_{0.90}$, respectively. The common d band (and therefore its Pd and Cu components) moves closer to ϵ_F on increasing the palladium concentration. We have marked the top of the Cu and Pd d bands in Figs. 2–7 (upper left-hand panel) and have tabulated it in Table I. We see both the Cu and Pd d -band edges moving closer to ϵ_F : the d -band edge of palladium in $\text{Cu}_{0.95}\text{Pd}_{0.05}$ is 1.3 eV below ϵ_F and moves to 0.1 eV above ϵ_F in $\text{Cu}_{0.10}\text{Pd}_{0.90}$. In $\text{Cu}_{0.95}\text{Pd}_{0.05}$ the copper d -band edge has already moved up, compared to its position in pure copper, to 1.5 eV below ϵ_F , and in $\text{Cu}_{0.10}\text{Pd}_{0.90}$ it is 0.3 eV below ϵ_F . The bandwidth of the high-density-of-states region of the copper d bands remains constant (2.1 eV) throughout the whole concentration range, even though the lattice constant increases by 5%, and the palladium d -band width increases from 4.4 eV in $\text{Cu}_{0.95}\text{Pd}_{0.05}$ to 5.3 eV in $\text{Cu}_{0.10}\text{Pd}_{0.90}$.

The message of these detailed comments is illustrated

TABLE I. Tabulation of concentrations (c) and lattice parameters (a) at which SCF-KKR-CPA calculations were performed. Also tabulated are calculated values for N_α^{MT} and N_α^{WS} ($\alpha = \text{Cu}$ or Pd), the number of electrons inside the muffin-tin (MT) sphere and Wigner-Seitz (WS) cell, respectively, $\epsilon_\alpha^{\text{r}}$ the resonance-energy positions for the Cu and Pd potentials, ϵ_F the Fermi energy (measured with respect to the muffin-tin zero), $\epsilon_F - \epsilon_\alpha^{\text{BE}}$, where $\epsilon_\alpha^{\text{BE}}$ is the position of the upper edge of the (Cu; Pd) d -band edge (BE), and W_α the Cu- and Pd-component d -band width.

c at. % Cu	a (a.u.)	$N_{\text{Cu}}^{\text{MT}}$	$N_{\text{Pd}}^{\text{MT}}$	$N_{\text{Cu}}^{\text{WS}}$	$N_{\text{Pd}}^{\text{WS}}$	ϵ_F^{Cu} (Ry)	ϵ_F^{Pd} (Ry)	ϵ_F (Ry)	$\epsilon_F - \epsilon_{\text{Cu}}^{\text{BE}}$ (eV)	$\epsilon_F - \epsilon_{\text{Pd}}^{\text{BE}}$ (eV)	W_{Cu} (eV)	W_{Pd} (eV)
95	6.858	10.34	9.07	11.01	9.81	0.404	0.336	0.620	-1.5	-1.3	2.0	4.4
75	6.957	10.38	9.10	11.05	9.84	0.423	0.348	0.615	-1.2	-0.7	2.1	4.9
60	7.041	10.42	9.14	11.06	9.91	0.430	0.354	0.600	-0.9	-0.4	2.1	5.0
50	7.090	10.50	9.17	11.07	9.93	0.433	0.363	0.595	-0.5	0.0	2.1	5.1
25	7.206	10.52	9.24	11.11	9.96	0.452	0.374	0.597	-0.4	0.1	2.1	5.2
10	7.219	10.54	9.28	11.13	9.99	0.459	0.374	0.599	-0.3	0.1	2.1	5.3

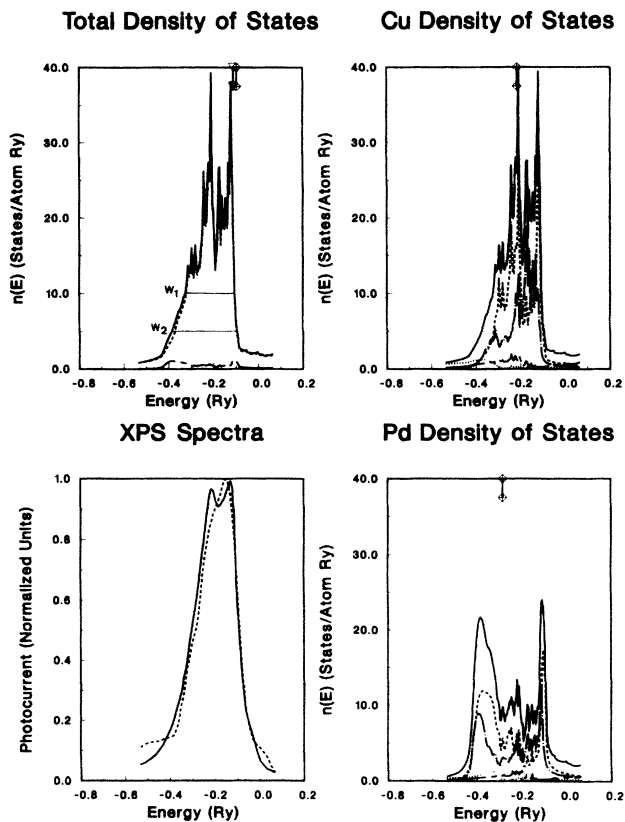


FIG. 2. Total and component densities of states and XPS spectra for $\text{Cu}_{0.95}\text{Pd}_{0.05}$ alloys plotted as a function of energy with respect to the Fermi energy. Upper left: the total density of states (solid line), the contribution from Cu sites (dotted—long-dashed line), and the contribution from Pd sites (dashed line). Upper right: the total densities of states (not concentration weighted) on a Cu site (solid line), the t_{2g} (d) component (dashed line), the e_g (d) component (dotted—short-dashed line), the t_{1u} (p) component (dotted—long-dashed line), and the a_{1g} (s) component (dotted—line). Lower right: same as upper right except for a Pd site. Lower left: calculated (solid line) and measured (dashed line) XPS spectra. The experimental results are those of Ref. 1.

dramatically by the local density of states (LDOS) on the impurity site at the two extremes of the concentration range. In $\text{Cu}_{0.95}\text{Pd}_{0.05}$ (Fig. 2, lower right-hand panel) the palladium LDOS is dominated by two strong peaks spanning the copper d bands. Neither of these peaks is located at the palladium d -resonance energy; indeed, in test calculations with *ad hoc* potentials we have found that this two-peak structure is quite insensitive to the position of the palladium resonance. In tight-binding language the situation is that the disorder in the off-diagonal hopping integrals is more important than the disorder in the diagonal site energies, and the two peaks are to be associated with bonding and antibonding states formed from the palladium d level and those on the surrounding copper atoms. The total width of the palladium DOS is large, due to just this strong hybridization. As mentioned above, non-self-consistent calculations place this structure too high in energy, resulting in a charge depletion of approximately one electron on the palladium sites. The ef-

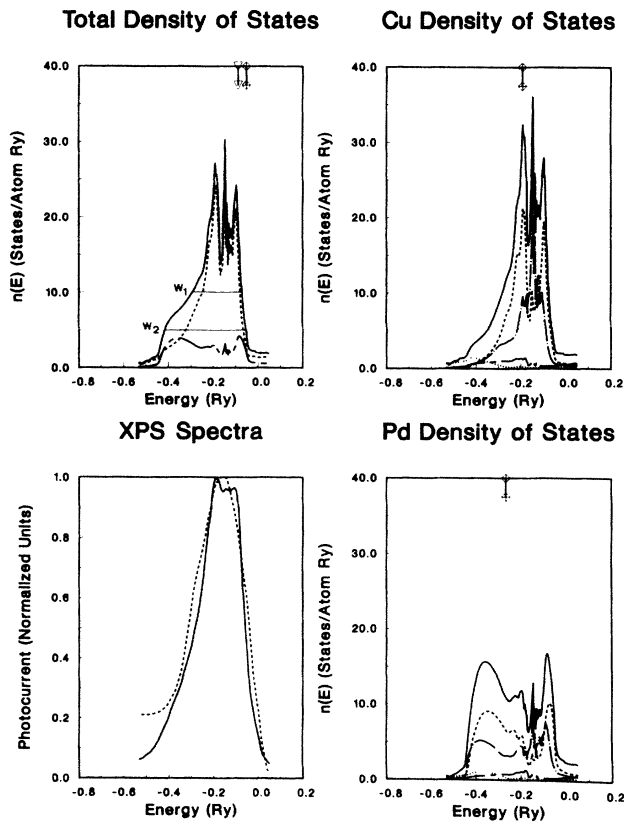


FIG. 3. Total and component densities of states and XPS spectra for $\text{Cu}_{0.75}\text{Pd}_{0.25}$ alloys. The key is as in Fig. 2.

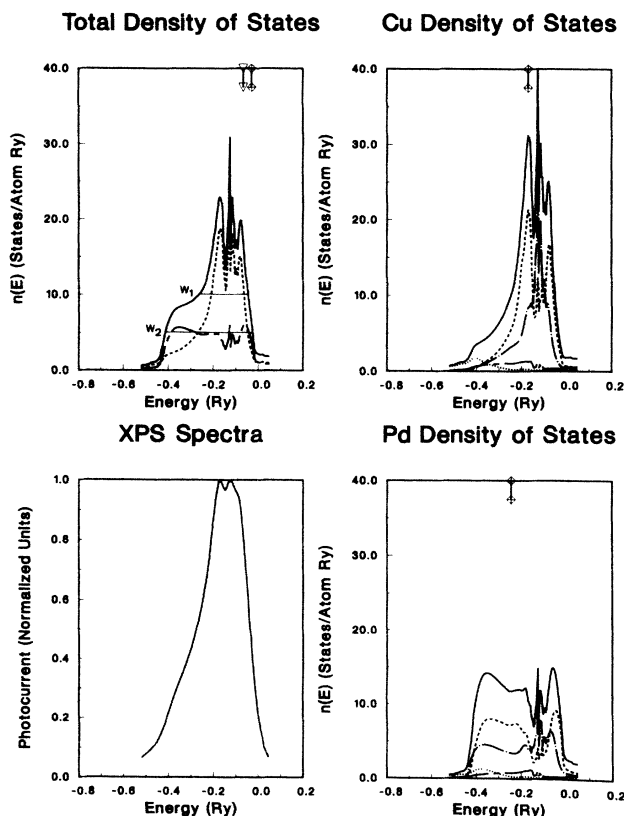


FIG. 4. Total and component densities of states and XPS spectra for $\text{Cu}_{0.60}\text{Pd}_{0.40}$ alloys. The key is as in Fig. 2.

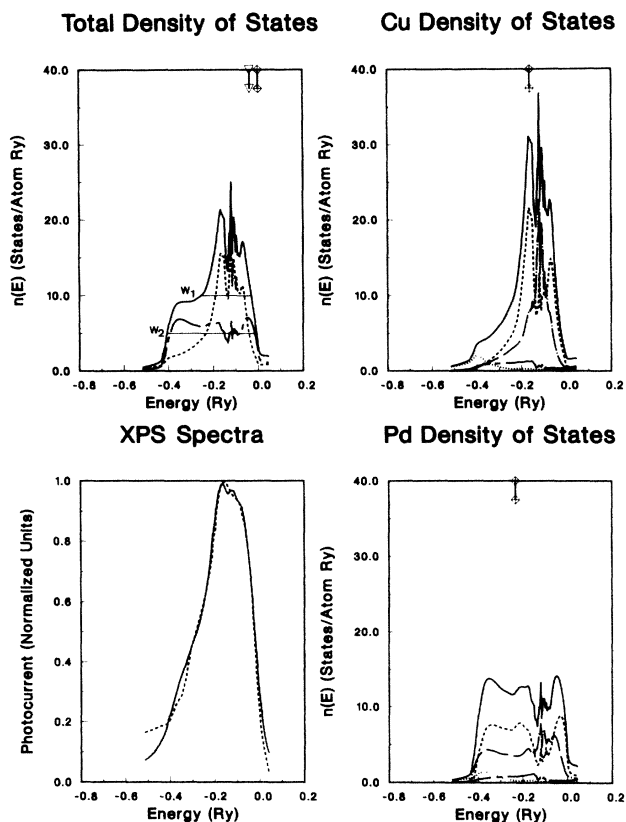


FIG. 5. Total and component densities of states and XPS spectra for $\text{Cu}_{0.50}\text{Pd}_{0.50}$ alloys. The key is as in Fig. 2.

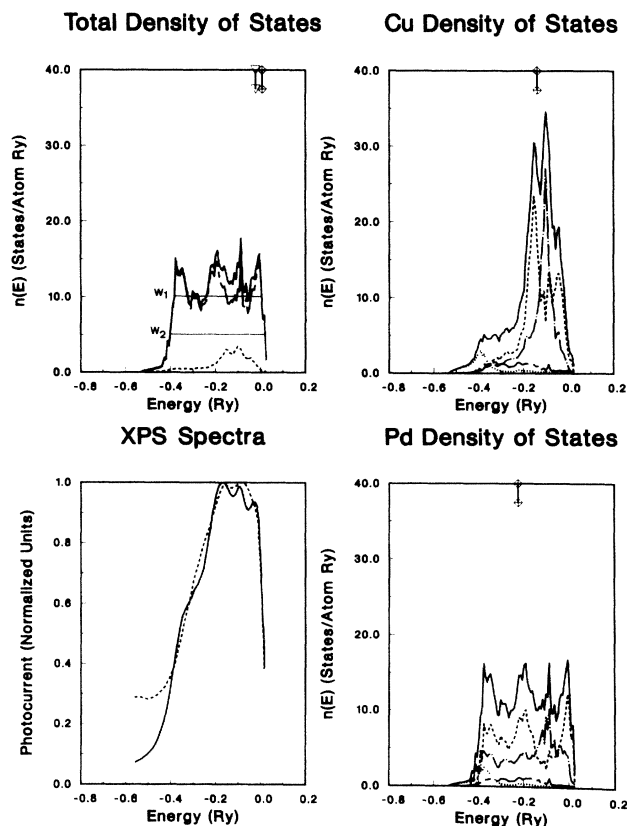


FIG. 7. Total and component densities of states and XPS spectra for $\text{Cu}_{0.10}\text{Pd}_{0.90}$ alloys. The key is as in Fig. 2.

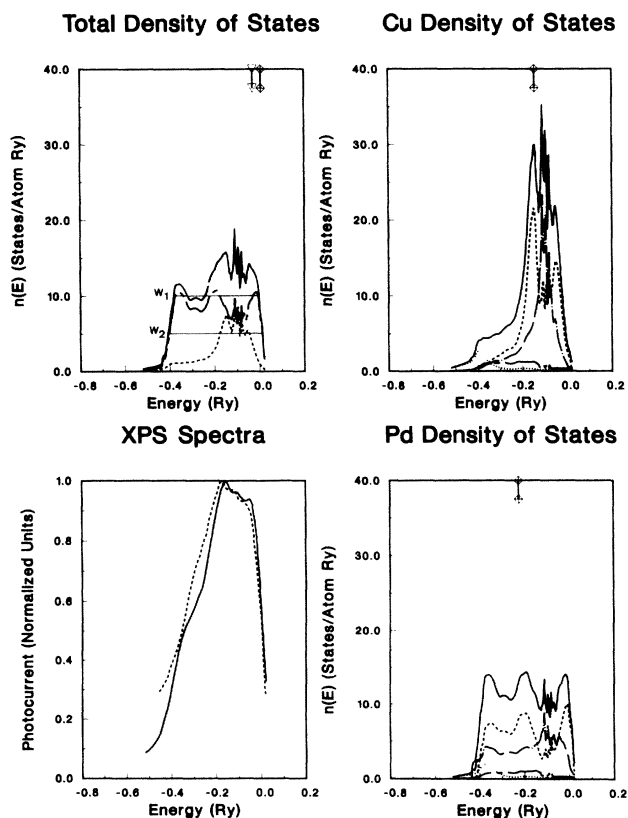


FIG. 6. Total and component densities of states and XPS spectra for $\text{Cu}_{0.25}\text{Pd}_{0.75}$ alloys. The key is as in Fig. 2.

fect of self-consistency is to lower the energy of palladium d states in such a way that local charge neutrality is (almost) obtained (Table I). At the opposite end of the concentration range we see that the copper LDOS in $\text{Cu}_{0.10}\text{Pd}_{0.90}$ (Fig. 7, upper right-hand panel) is likewise grossly deformed from that of pure copper. At low energies extra weight in the d LDOS is introduced by the strong hybridization with the surrounding palladium d states. This means that in order to maintain local charge neutrality again, the whole copper d band system has to move up towards the Fermi level and, in fact, approach it very closely.

From the foregoing discussion we conclude that the existence of strong off-diagonal disorder in an alloy system will, in general, imply that self-consistency will be important; the hybridization of the Cu and Pd d bands changes the number of states on the constituents, and the respective potentials need to be realigned with respect to each other to minimize charge transfer. This, in turn, will change the hybridization, and so on. This hybridization will be sensitive to composition and arrangement. A measure of the change in the potential functions with concentration is the splitting of the d resonances. We find from Table I that the splitting remains roughly constant throughout the whole concentration range; the effects of changing composition and lattice constant cancel out. From the preceding argument we might also anticipate that a SCF calculation for a surface of Cu-Pd might give different answers; we will return to this point later.

The Pd and Cu densities of states for $\text{Cu}_{0.75}\text{Pd}_{0.25}$ and $\text{Cu}_{0.95}\text{Pd}_{0.05}$ extrapolate nicely to previous SCF calculations by Braspenning *et al.* of a palladium impurity in a copper host.²⁷ The high-energy palladium *d* peak narrows from 0.6 eV in $\text{Cu}_{0.75}\text{Pd}_{0.25}$ to 0.35 eV in $\text{Cu}_{0.95}\text{Pd}_{0.05}$; the impurity calculations give 0.2 eV. However, we do not get a splitting of this peak into sharp subpeaks as seen in the impurity calculations. Presumably this is a feature of the very dilute limit. We think it misleading to call the high-energy palladium peak a virtual bound state, as the above authors do, since it lies far above the palladium resonance, and the palladium impurity has states throughout the energy range of the copper *d* states.

The effects of off-diagonal randomness can be seen by comparing our calculations with previous tight-binding CPA calculations³ in which only diagonal randomness was considered and which used overlap integrals appropriate to pure Pd (Cu) at the lattice spacing of the alloy in question for treating Pd (Cu)-rich alloys. In those calculations it was found that the *d*-band width increased from 4.0 eV in pure palladium to 6 eV in $\text{Cu}_{0.75}\text{Pd}_{0.25}$ (smaller lattice constant), and the copper bandwidth decreases from 2 eV in pure copper to 1.6 eV in $\text{Cu}_{0.60}\text{Pd}_{0.40}$ (larger lattice constant). From Table I we see that in our calculation, which includes diagonal and off-diagonal randomness on equal footing, the main copper *d*-band width remains constant throughout the whole concentration range, and the palladium *d*-band width decreases on increasing copper concentration. In the tight-binding calculations on palladium-rich alloys a nearly-split-off copper *d* band at 5 eV below ϵ_F was found (we find the Cu *d* band at 2.2 eV below ϵ_F), and for copper-rich alloys split-off palladium *d* bands at 1.1 eV below ϵ_F in $\text{Cu}_{0.90}\text{Pd}_{0.10}$ and 0.4 eV below ϵ_F in $\text{Cu}_{0.60}\text{Pd}_{0.40}$ were also found.

This comparison confirms the suspicion that tight-binding CPA calculations are an unreliable guide in systems for which off-diagonal randomness is important, simply because this effect is not treated in the model.²⁸ The KKR-CPA does not suffer from this defect and is, therefore, able to describe such systems quantitatively; indeed, this was a prime motivation behind the development of the KKR-CPA. Cu-Pd seems to have been the first alloy to be treated by the KKR-CPA in which diagonal disorder does not dominate. Cu-Ni and Ag-Pd are, as mentioned above, classic split-band systems in which the bandwidths of the pure components are similar and off-diagonal disorder small. For Cu-Zn the pure Cu and Zn bandwidths are very different,^{29,30} but the difference in the *d*-resonance energies (or site energies) is even greater. In Nb-Mo the diagonal disorder is small;³¹ however, the bandwidths for pure Nb and pure Mo are very similar. This results in rigid-band (or rather virtual-crystal) behavior, i.e., a single common *d* band whose shape is relatively insensitive to concentration. Cu-Pd is the only alloy so far examined in which off-diagonal disorder is large and diagonal disorder somewhat smaller, producing a common *d* band whose shape is a strongly varying function of concentration.

As we have mentioned previously, in a recent non-self-consistent KKR-CPA calculation,⁶ essentially the same

results as the SCF-KKR-CPA are obtained. However, in these calculations the authors substantially adjusted their Mattheiss-prescription potential functions in an *ad hoc* manner in order to fit angle-resolved photoemission data. In particular, they had to shift the palladium potential rigidly down by 2.45 eV with respect to the copper potential. They obtain for the two concentrations considered, $\text{Cu}_{0.95}\text{Pd}_{0.05}$ and $\text{Cu}_{0.85}\text{Pd}_{0.15}$, no split-off palladium band. They too find a strong hybridization of the Pd and Cu *d* bands. However, one of the effects of self-consistency is to move both Cu and Pd bands closer to ϵ_F (see Table I). In the non-self-consistent calculation only the palladium *d*-band edge moves, from 1.5 eV below ϵ_F ($\text{Cu}_{0.95}\text{Pd}_{0.05}$) to 0.8 eV below ϵ_F ($\text{Cu}_{0.85}\text{Pd}_{0.15}$), while the copper *d*-band edge remains at about 2 eV below ϵ_F .

To conclude this section we show in Table II the values of the following quantities: the Fermi energies with respect to the muffin-tin zero, the partial and the total density of states, the phase shifts, and the single-scatterer density of states, all evaluated at ϵ_F . In Fig. 8 we display the electronic specific-heat coefficient γ obtained with the use of our total density of states and neglecting the mass-enhancement factor. The calculated γ has the same qualitative behavior as the measured γ .¹⁸ By comparing the two curves we derive values for the mass-enhancement parameter λ . These rise monotonically from values below 0.1 at the copper-rich concentration side to 0.65 near pure palladium.

The results are consistent with the calculation for the pure systems.^{32,33} Between 30% and 60% of palladium, our λ estimates are based on the interpolated γ values of Sato *et al.*¹⁸ A shoulder in λ at this concentration (Fig. 8) might therefore be spurious, caused by an overestimation of γ . To clarify this point, specific-heat measurements

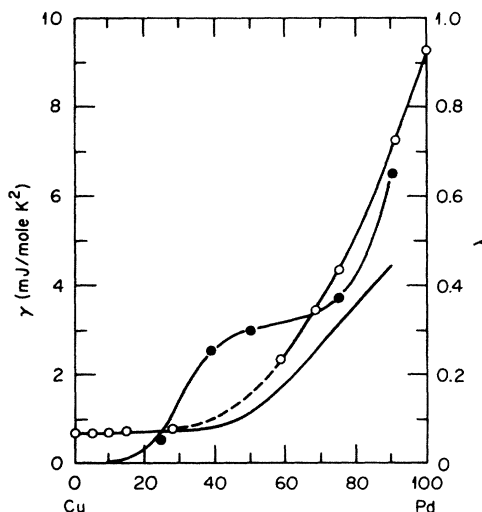


FIG. 8. Calculated (solid line) and measured (open circles) low-temperature specific-heat coefficient γ . The experimental results are those of Ref. 18. The dashed curve is our interpolation of the experimental results through the two-phase region (Ref. 18). The calculated results do not include the electron-phonon mass-enhancement factor $(1 + \lambda)$. The solid circles indicate the values of λ obtained by dividing the experimental values by the calculated values.

TABLE II. Tabulation, for the six alloys calculated, of the Fermi energy ϵ_F and calculated values at ϵ_F of the total and Cu- and Pd-component densities of states. Also tabulated are the phase shifts and single-scatterer densities obtained at ϵ_F for single Cu and Pd muffin-tin potentials.

Alloy	Fermi energy (Ry)	Total DOS (states/Ry spin atom)	Partial DOS per site		Single-scatterer partial DOS		Phase shifts				
			Cu site	Pd site	Cu site	Pd site	Cu site	Pd site			
Cu _{0.95} Pd _{0.05}	0.6204	2.00	<i>s</i>	0.268	0.213	<i>s</i>	0.498	0.398	<i>s</i>	-0.0908	-0.0399
			<i>p</i>	0.689	0.494	<i>p</i>	0.886	0.596	<i>p</i>	0.0862	-0.0726
			<i>t_{2g}</i>	0.625	1.01	<i>t_{2g}</i>	0.672	0.543	<i>d</i>	2.978	2.818
			<i>e_g</i>	0.398	0.700	<i>e_g</i>	0.447	0.814			
Cu _{0.75} Pd _{0.25}	0.6150	2.04		0.259	0.202		0.513	0.410		-0.1302	-0.408
				0.527	0.432		0.889	0.623		-0.0652	-0.0745
				0.658	1.10		0.836	0.930		2.960	2.800
				0.400	0.698		0.556	0.621			
Cu _{0.60} Pd _{0.40}	0.6004	2.16		0.239	0.185		0.531	0.423		-0.1426	-0.4076
				0.472	0.356		0.894	0.639		0.0544	-0.0726
				0.672	1.36		0.970	1.01		2.951	2.797
				0.429	0.781		0.645	0.676			
Cu _{0.50} Pd _{0.50}	0.5953	3.44		0.207	0.179		0.539	0.430		-0.155	-0.414
				0.372	0.291		0.897	0.649		0.047	-0.0747
				0.951	3.44		1.06	1.09		2.944	2.788
				0.442	0.998		0.706	0.729			
Cu _{0.25} Pd _{0.75}	0.5970	9.06		0.189	0.150		0.555	0.442		-0.204	-0.441
				0.329	0.271		0.907	0.678		0.022	-0.0855
				2.67	8.45		1.27	1.195		2.925	2.774
				0.738	1.90		0.846	0.798			
Cu _{0.10} Pd _{0.90}	0.5990	12.68		0.184	0.146		0.571	0.456		-0.210	-0.435
				0.311	0.260		0.924	0.703		0.016	0.081
				2.71	10.36		1.445	1.26		2.915	2.772
				0.870	2.89		0.962	0.841			

for rapidly quenched samples in this concentration range are in progress.³⁴ Furthermore, nothing in the Fermi-energy data (Table II), when used in Gaspari-Gyorffy-type theory,³⁵ indicates a shoulder in λ . However, we do not give a full evaluation of λ in the present paper because we did not evaluate the \mathcal{L} contributions to the electronic part of λ , and we did not consider the phonons in our study. The mass enhancement of Cu_cPd_{1-c} alloys is similar to that of Ag_cPd_{1-c} alloys.³⁶ Thus the fact that the copper *d* density of states is enhanced in palladium-rich Cu_cPd_{1-c} alloys compared with the silver *d* density of states in Ag_cPd_{1-c} does not appear to affect the λ values.

III. THE XPS CROSS SECTIONS

We have evaluated the XPS valence-electron cross sections in the one-particle approximation as described in detail previously.⁷ As the photon energy $\hbar\omega$, we took 1364 eV, corresponding to the Mg *K* α line. The cross section σ in this approach is determined by the imaginary part of the valence-electron Green's function and the Green's function of the excited electron. The electron-photon cou-

pling contains the spatial derivatives $\partial V^{A(B)}(r)/\partial r$ of the alloy potentials (A or $B \equiv$ Cu or Pd). In a real-space representation, both site-diagonal and site-off-diagonal parts of the valence-electron Green's function contribute to the photoemission cross section. Whereas the site-diagonal quantities may be expressed in terms of the partial densities of states, the interpretation of the site-off-diagonal terms is less obvious. In fact, at low photon energies they contribute very strongly, leading to \mathbf{k} -conserving "direct-transition"-like features in photoemission.³⁷ However, our previous investigation of Ag-Pd alloys showed that, due chiefly to the high energies of the excited electrons, a local approximation consisting of omitting the site-off-diagonal contributions is rather accurate. This has proved to hold for the Cu_cPd_{1-c} alloys as well, and so we restrict the discussion in this paper to the local approach.

At high energies multiple scattering can be neglected, and the photoelectron wave function can be approximated in the neighborhood of any atom i by a solution of the Schrödinger equation for a single $V^i(r)$. We call this the single-scatterer final state.³⁸ Within the KKR-CPA, averaging over alloy configurations is then trivial, and the final expression to be evaluated is

$$\sigma(E + \hbar\omega) = \frac{4}{9} \left(\frac{e\pi}{\omega} \right)^2 \left[\frac{2(E + \hbar\omega)}{mc^2} \right]^{1/2} \sum_{\substack{\lambda, \mu, \\ \lambda', \mu'}} \sum_{\mu''} (g_{\lambda\lambda'}^{\mu\mu''} A_{\mu''})^2 [c |M_{ll'}^{\text{Cu}}(E)|^2 n_{\lambda}^{\text{Cu}}(E) + (1-c) |M_{ll'}^{\text{Pd}}(E)|^2 n_{\lambda}^{\text{Pd}}(E)], \quad (1)$$

where λ, μ label the cubic harmonics corresponding to angular momentum l [i.e., $s, p, d(e_g), d(t_{2g}),$ etc.], $g_{\lambda\lambda'}^{\mu\mu''}$ is a Gaunt number for the cubic harmonics, $A_{\mu''}$ is a component of the vector potential, $n_{\lambda}^{\text{Cu}}(E)$ is a component of the copper local density of states, and $M_{ll'}^{\text{Cu}}(E)$ is a matrix element of $dV^{\text{Cu}}(r)/dr$ between solutions of the copper single-site Schrödinger equation at energy E , and angular momentum l , and at energy $E + \hbar\omega$ and angular momentum l' (a full definition of these quantities is given in Ref. 7), the corresponding quantities for a palladium potential have the superscript Pd. From the above expression it may be seen that it is hard to draw unequivocal conclusions about the partial DOS from XPS measurements alone, unless one particular partial DOS outweighs the others or the system shows split-band behavior (neither of these situations applies for $\text{Cu}_c\text{Pd}_{1-c}$ alloys). Moreover, experimental data are subject to appreciable lifetime and instrumental broadening; it is also hard to subtract the background from the measurements in a well-founded manner.⁷

As in the $\text{Ag}_c\text{Pd}_{1-c}$ case, it turns out that for $\text{Cu}_c\text{Pd}_{1-c}$ the single-scatterer final state deviates markedly from a plane wave. This leads to changes of the matrix elements in comparison to the plane-wave approximation. The lower left-hand panel in Figs. 2–7 shows the calculated σ 's based on the single-scatterer final state and broadened by folding with Lorentzians of half-widths

$$\Gamma = A(\epsilon - \epsilon_F)^2 / (\epsilon_F - \epsilon_B)^2.$$

Here, ϵ_B is the energy of the bottom of the band, and ϵ_F is the Fermi energy. For A we chose 1 eV. The instrumental broadening was taken into account by folding this result again with a Gaussian of 0.25 eV half-width. In the same picture we include the experimental results⁴ for comparison.

No effort was made to subtract a background from the experimental data, but the theoretical and experimental upper d -band edges were aligned to facilitate comparison (this involved shifts of, at most, 0.2 eV). It can be seen that in overall shape and width our calculations are in remarkably good agreement with experiment. Even some of the fine structure remaining in the broadened theoretical spectra seems to be reflected in the data. In Table III we

TABLE III. Comparison of widths (W) and upper-band-edge (BE) positions ($\epsilon_F - \epsilon_{\text{BE}}$) extracted from the calculated and measured XPS spectra shown in Figs. 2–7.

at. % Cu	W_{theor}	W_{expt}	$(\epsilon_F - \epsilon_{\text{BE}})_{\text{theor}}$	$(\epsilon_F - \epsilon_{\text{BE}})_{\text{expt}}$
95	2.9	2.7	1.3	1.3
75	3.0	3.8	0.8	0.6
60	3.2		0.5	
50	3.5	3.5	0.3	0.3
25	4.8	4.9	-0.2	-0.2
10	5.1	4.9	-0.2	-0.2

compare the calculated and measured widths [full width at half maximum (FWHM)] and positions of the upper d -band edges (without the shift applied in Figs. 2–7). The quantitative agreement is again very good (apart from the width for the $\text{Cu}_{0.75}\text{Pd}_{0.25}$ alloy, whose measured value appears somewhat anomalous). The structure in the XPS cross sections clearly reflects the densities of states, with the energy dependence of the matrix elements enhancing the high-energy peaks.

We now comment on previous attempts⁴ to estimate experimentally the individual Cu and Pd contributions to the DOS by applying a subtraction procedure to the data. The same method has been applied to palladium-rich alloys.² In the experimental subtraction procedure it is assumed that the contribution of the majority component to σ is the undeformed (concentration-weighted) cross section of the corresponding pure metal, and by subtraction the contribution of the minority component is extracted. Our results provide the possibility to test the validity of this approach. Note in particular that Figs. 2–7 show a deformation and movement toward the Fermi level of the upper edge of the copper d band as palladium is alloyed to copper. Thus, if the DOS of pure copper is subtracted from that of a copper-rich alloy, the difference spectrum will show negative features toward the lower part of the d band and, most strikingly, a large positive peak just above the pure copper d bands. If one identified this difference spectrum with the local palladium density of states, one would naturally conclude that palladium formed a virtual bound state in the alloy, and indeed, this has hitherto been the interpretation of the XPS data in Cu-Pd.⁴ While such an interpretation would be quite reasonable for true split-band systems like Cu-Ni and Ag-Pd, it is clearly fallacious for Cu-Pd, whose d band moves relative to E_F , as well as deforming, as the concentration changes.

It should be mentioned that Nemoshkalenko *et al.*³ give a theory for the XPS cross section, including matrix-element effects, in their papers on $\text{Cu}_c\text{Pd}_{1-c}$ alloys. However, their application of the tight-binding interpolation scheme neglects off-diagonal randomness, and they obtain split-band behavior. However, they compare their results to experiments of low resolution and, accordingly, they impose a large broadening on their theoretical curves. The dips between their calculated Cu and Pd d bands are washed out in this manner, and they obtain compatibility with those experiments. Significant discrepancies, however, arise if one compares their results with the high-resolution experiments of Ref. 4.

We summarize this comparison of theoretical and experimental XPS cross sections by stressing the following three general features of the data. First, there is no obvious split-band behavior at any concentration—only one d band is visible in each alloy; second, the upper d -band edge moves toward the Fermi energy as the palladium content increases; and third, at the same time, spectral weight builds up toward the lower part of the d band.

These features in themselves lend experimental support to our picture of the underlying electronic structure. They correspond to our findings that no palladium virtual bound state is formed, but rather that strong Cu-Pd mixing leads to a single d band which moves toward ϵ_F as the palladium concentration increases, and whose palladium component has a growing number of states around the lower d -band edge. Given this, our first-principles evaluations of σ then provide convincing confirmation of the details of the KKR-CPA calculations.

IV. CONCLUSIONS

Our SCF-KKR-CPA calculations show that Cu-Pd is not a split-band system—it has a common d band at all concentrations, but, in contrast to the rigid-band model, the two local densities of states are quite different and vary strongly with composition. We have argued that this is a characteristic of alloys dominated by off-diagonal disorder, and that self-consistency is especially important for such systems.

We obtain good agreement between our first-principles calculations of the XPS spectra and experiment, and show that the virtual-bound-state interpretation of the data is wrong. In soft-x-ray-emission experiments one can observe the Cu and Pd local densities of states separately. If a palladium virtual bound state were formed, its local density of states would behave quite differently, as a function of concentration from our calculation (see, for example, the data for Cu-Ni alloys).³⁹ We plan to report on this key topic in a later publication.

Very recent angle-resolved photoemission data for Cu-rich Cu-Pd alloys⁴⁰ clearly show the d bands approaching the Fermi level as the palladium content increases. They also show a peak above the copper d bands, roughly where the nickel virtual bound state occurs in Cu-rich Cu-Ni alloys. Our Bloch spectral functions and preliminary first-

principles calculations of the photocurrent⁴¹ show that this feature is not present in the bulk spectral density of random Cu-Pd, in disagreement with a previous suggestion.⁶ At present we have no quantitative explanation of this interesting result. It is possible that the short-range order known to occur in this alloy may introduce new features into the spectral density. On the other hand, the argument in Sec. II suggests that the surface may radically perturb the electronic structure in its vicinity. Louie⁴² has found that the d -band local density of states in the (111) surface layer of pure palladium is 16% narrower than in the bulk. In the alloy this would tend to reduce the importance of off-diagonal disorder, thus allowing the palladium d band to rise relative to that of copper. In such circumstances a palladium virtual bound state in the surface layer might become a possibility. Of course, this speculation needs to be checked by further calculations (now in progress), and it may well be that a full description of the surface electronic structure of Cu-Pd alloys will require a careful consideration of both concentration correlations and self-consistency.

However, on the basis of our account of the XPS and low-temperature specific-heat data, we believe our description of the bulk electronic structure of the random alloy to be quantitatively reliable.

ACKNOWLEDGMENTS

We thank Dr. L. Ilver, Dr. P.-O. Nilsson, Dr. R. G. Jordan, Dr. B. L. Gyorffy, and Dr. J. E. Inglesfield for useful discussions. One of us (G.M.S.) would like to thank the Science and Engineering Research Council (SERC) for the support and hospitality extended during a sabbatical leave taken in Daresbury. The work of G.M.S. was also supported in part by the Division of Materials Sciences, U.S. Department of Energy, under Contract No. DE-AC05-84OR21400 with Martin Marietta Energy Systems, Inc.

¹J. Hedman, M. Klasson, R. Nilsson, C. Nordling, M. F. Sorokina, O. I. Kljusnikov, S. A. Nemnonov, V. A. Trapeznikov, and V. G. Zynjanov, *Phys. Scr.* **4**, 195 (1971).

²S. Hufner, G. K. Wertheim, and J. H. Wernick, *Solid State Commun.* **17**, 1585 (1975).

³V. V. Nemoshkalenko, V. G. Aleshin, V. M. Pessa, and M. G. Chudinov, *Phys. Scr.* **11**, 387 (1975).

⁴N. Martensson, R. Nyholm, H. Calén, J. Hedman, and B. Johansson, *Phys. Rev. B* **24**, 1725 (1981).

⁵P. Weightman, P. T. Andrews, G. M. Stocks, and H. Winter, *J. Phys. C* **16**, L81 (1983).

⁶R. S. Rao, A. Bansil, H. Asonen, and M. Pessa, *Phys. Rev. B* **29**, 1713 (1984).

⁷H. Winter, P. J. Durham, and G. M. Stocks, *J. Phys. F* **14**, 1047 (1984).

⁸M. Hansen, *Constitution of Binary Alloys* (McGraw-Hill, New York, 1958).

⁹P. Politis (private communication).

¹⁰K. Ohshima and D. Watanabe, *Acta Crystallogr. Sect. A* **29**, 520 (1973).

¹¹F. Ducastelle and F. Gautier, *J. Phys. F* **6**, 2039 (1976).

¹²A. Bieber, F. Gautier, G. Treglia, and F. Ducastelle, *Solid*

State Commun. **39**, 149 (1981).

¹³B. L. Gyorffy and G. M. Stocks, *Phys. Rev. Lett.* **50**, 374 (1983).

¹⁴L. F. Mattheiss, *Phys. Rev. B* **1**, 373 (1970).

¹⁵A. J. Pindor, W. M. Temmerman, B. L. Gyorffy, and G. M. Stocks, *J. Phys. F* **10**, 2617 (1980).

¹⁶W. M. Temmerman, B. L. Gyorffy, and G. M. Stocks, *J. Phys. F* **8**, 2461 (1978).

¹⁷G. M. Stocks, W. M. Temmerman, and B. L. Gyorffy, *Phys. Rev. Lett.* **41**, 34 (1978).

¹⁸Y. Sato, J. M. Silverstein, and L. E. Toth, *Phys. Rev. B* **14**, 1402 (1970).

¹⁹S. Kobayashi, K. Asayama, and J. Itoh, *J. Phys. Soc. Jpn.* **18**, 1735 (1963).

²⁰J. Itoh, K. Asayama, and S. Kabayashi, *Proc. Colloq. Ampère* **13**, 162 (1965).

²¹A. Narath and H. T. Weaver, *Phys. Rev. B* **3**, 616 (1971).

²²A. Bansil, *Phys. Rev. Lett.* **41**, 1670 (1978).

²³G. M. Stocks and H. Winter, *Z. Phys. B* **46**, 95 (1982).

²⁴H. Winter and G. M. Stocks, *Phys. Rev. B* **27**, 882 (1983).

²⁵Z. Szotek, B. L. Gyorffy, G. M. Stocks, and W. M. Temmerman, *J. Phys. F* **14**, 2571 (1984).

- ²⁶U. von Barth and L. Hedin, *J. Phys. C* **5**, 1629 (1972).
- ²⁷P. J. Braspenning, R. Zeller, P. H. Dedrichs, and A. Lodder, *J. Phys. F* **12**, 105 (1982).
- ²⁸We have recently learned of a new tight-binding-like scheme [J. Kudmouky and J. Masek (unpublished)] that appears to overcome some of the difficulties associated with the treatment of off-diagonal disorder and is able to give reasonable results for the $\text{Cu}_c\text{Pd}_{1-c}$ alloy system.
- ²⁹J. S. Faulkner and G. M. Stocks, *Phys. Rev. B* **23**, 5628 (1981).
- ³⁰A. Bansil, *Phys. Rev. B* **20**, 4035 (1979).
- ³¹E. S. Giliano, R. Ruggeri, B. L. Gyorffy, and G. M. Stocks, in *Transition Metals 1977*, edited by M. J. G. Lee, J. M. Perz, and E. Fawcett (IOP, Bristol, England, 1978), p. 410.
- ³²D. A. Papaconstantopoulos, L. L. Boyer, B. M. Klein, A. R. Williams, V. Moruzzi, and J. F. Janak, *Phys. Rev. B* **15** 4221 (1977).
- ³³W. H. Butler, *Phys. Rev. B* **15**, 5267 (1977).
- ³⁴R. Ahrens, H. Keiber, C. Politis, and H. Wühl, in *Europphysics Conference Abstract 9A*, Proceedings of the 5th General Conference of the Condensed Matter Division of the European Physical Society, edited by S. Methfessel, p. PWE-5-094, 1985 (unpublished), report new measurements of γ confirming that the interpolated values of γ taken from Sato *et al.* are indeed too large, and, therefore, that the hump in λ for $C \sim 0.4$ is spurious.
- ³⁵G. D. Gaspari and B. L. Gyorffy, *Phys. Rev. Lett.* **28**, 801 (1972).
- ³⁶B. L. Gyorffy, A. J. Pindor, and W. M. Temmerman, *Phys. Rev. Lett.* **43**, 1343 (1979).
- ³⁷P. J. Durham, *J. Phys. F* **11**, 2475 (1981).
- ³⁸N. J. Shevchik and D. Liebowitz, *Phys. Rev. B* **16**, 2395 (1977).
- ³⁹P. J. Durham, D. Ghaleb, B. L. Gyorffy, C. F. Hague, J.-M. Mariot, G. M. Stocks, and W. M. Temmerman, *J. Phys. F* **9**, 1719 (1979).
- ⁴⁰See Ref. 30; L. Ilver and P.-O. Nilsson (private communication); R. Jordan and G. Schal (private communication).
- ⁴¹B. Genatempo and P. J. Durham (unpublished).
- ⁴²S. Louie, *Phys. Rev. Lett.* **40**, 1525 (1978).